Journal of the American Heart Association

ORIGINAL RESEARCH

Angiotensin II Disrupts Neurovascular Coupling by Potentiating Calcium Increases in Astrocytic Endfeet

Michaël Boily, MSc*; Lin Li, PhD*; Diane Vallerand, BSc; Hélène Girouard, PhD

BACKGROUND: Angiotensin II (Ang II), a critical mediator of hypertension, impairs neurovascular coupling. Since astrocytes are key regulators of neurovascular coupling, we sought to investigate whether Ang II impairs neurovascular coupling through modulation of astrocytic Ca^{2+} signaling.

METHODS AND RESULTS: Using laser Doppler flowmetry, we found that Ang II attenuates cerebral blood flow elevations induced by whisker stimulation or the metabotropic glutamate receptors agonist, 1S, 3R-1-aminocyclopentane-*trans*-1,3-dicarboxylic acid ($P<0.01$). In acute brain slices, Ang II shifted the vascular response induced by 1S, 3R-1-aminocyclopentane-*trans*-1,3-dicarboxylic acid towards vasoconstriction ($P<0.05$). The resting and 1S, 3R-1-aminocyclopentane-*trans*-1,3-dicarboxylic acid–induced Ca^{2+} levels in the astrocytic endfeet were more elevated in the presence of Ang II ($P<0.01$). Both effects were reversed by the AT1 receptor antagonist, candesartan ($P<0.01$ for diameter and $P<0.05$ for calcium levels). Using photolysis of caged Ca^{2+} in astrocytic endfeet or pre-incubation of 1,2-Bis(2-aminophenoxy)ethane-*N,N,N',N'*-tetra-acetic acid tetrakis (acetoxymethyl ester), we demonstrated the link between potentiated Ca^{2+} elevation and impaired vascular response in the presence of Ang II ($P<0.001$ and $P<0.05$, respectively). Both intracellular Ca^{2+} mobilization and Ca^{2+} influx through transient receptor potential vanilloid 4 mediated Ang II-induced astrocytic Ca^{2+} elevation, since blockade of these pathways significantly prevented the intracellular Ca^{2+} in response to 1S, 3R-1-aminocyclopentane-*trans*-1,3-dicarboxylic acid ($P<0.05$).

CONCLUSIONS: These results suggest that Ang II through its AT1 receptor potentiates the astrocytic Ca^{2+} responses to a level that promotes vasoconstriction over vasodilation, thus altering cerebral blood flow increases in response to neuronal activity.

Key Words: angiotensin II ■ astrocytes ■ calcium ■ neurovascular coupling ■ TRPV4

Hypertension exerts profound effects on cerebrovascular structures and functions[1,2] and is a key risk factor for dementia.[2–4] In patients with chronic untreated hypertension, a brain imaging study showed that the local neuronal regulation of cerebral blood flow (CBF) produced by cognitive tasks, a process termed neurovascular coupling (NVC), was altered.[5] The attenuated response was associated with a lower cognitive performance.[5] Angiotensin II (Ang II), a critical mediator of hypertension, has emerged as a culprit of impaired neurovascular regulation.[2,4,6] This peptide, classically recognized to be synthesized in the lung and released into the systemic circulation, can also be produced locally in the brain.[7] In addition, Ang II is known to cross the blood–brain barrier in experimental models of hypertension.[8,9] Both circulating and locally perfused Ang II disrupts NVC.[4,10] Interestingly, Ang II impairs NVC independently of its effect on blood pressure. Indeed, in the slow pressor model, this effect precedes mean arterial pressure elevation.[11] Long-term administration of phenylephrine to elevate blood pressure fails to alter NVC, whereas subpressor doses of Ang II (200

Correspondence to: Hélène Girouard, PhD, Department of Pharmacology and Physiology, Faculty of Medicine, Université de Montréal, Pavillon Roger-Gaudry, 2900 Édouard-Montpetit, Montréal, Québec H3T 1J4, Canada.E-mail: helene.girouard@umontreal.ca

†M. Boily and L. Li contributed equally.

Supplementary Materials for this article are available at https://www.ahajournals.org/doi/suppl/10.1161/JAHA.120.020608

For Sources of Funding and Disclosures, see page 12.

JAHA is available at: www.ahajournals.org/journal/jaha

CLINICAL PERSPECTIVE

What Is New?

- This study represents the first indication that angiotensin II could impair neurovascular coupling by increasing vascular tone through amplification of astrocytic Ca^{2+} signaling.

What Are the Clinical Implications?

- It is now recognized that to treat brain diseases, the whole neurovascular unit, including astrocytes and blood vessels, should be considered.
- It is known that age-associated brain dysfunctions and neurodegenerative diseases are improved by angiotensin receptor antagonists that cross the blood–brain barrier; therefore, results from the present study support the use of angiotensin receptor antagonists to normalize astrocytic and vascular functions in these diseases.
- Results from the present study may also imply that high cerebral angiotensin II may alter brain imaging signals evoked by neuronal activation.

Nonstandard Abbreviations and Acronyms

aCSF	artificial cerebrospinal fluid
Ang II	angiotensin II
CBF	cerebral blood flow
mGluR	metabotropic glutamate receptor
NVC	neurovascular coupling
***t*-ACPD**	1S, 3R-1-aminocyclopentane-*trans*-1,3-dicarboxylic acid
TRPV4	transient receptor potential vanilloid 4
XC	xestospongin C

ng/kg per min) still impair NVC.[11,12] In addition, Ang II AT1 receptor blockers that cross the blood–brain barrier show beneficial effects on NVC in hypertension, stroke, and Alzheimer disease models.[13–17] Although many mechanisms have been proposed to explain the effects of Ang II on NVC, the molecular pathways remain unclear. It is known that Ang II at low concentrations does not acutely affect neuronal excitability or smooth muscle cell reactivity but still impairs NVC,[4] suggesting that astrocytes may play a central role in the acute Ang II–induced NVC impairment.

Astrocytes are uniquely positioned between synapses and blood vessels, surrounding both neighboring synapses with their projections and most of the arteriolar and capillary abluminal surface with their endfeet. Functionally, astrocytes perceive neuronal activity by responding to neurotransmitters, then transducing signals to the cerebral microcirculation.[18–21] In the somatosensory cortex area, astrocytic Ca^{2+} signaling has been considered to play a role in NVC.[22,23] Interestingly, it seems that the level of intracellular Ca^{2+} concentration ($[Ca^{2+}]_i$) in the endfoot determines the response of adjacent arterioles: moderate $[Ca^{2+}]_i$ increases in the endfoot induce parenchymal arteriole dilation, whereas high $[Ca^{2+}]_i$ results in constriction.[18] Among mechanisms known to increase astrocytic Ca^{2+} levels in NVC is the activation of inositol 1,4,5-trisphosphate receptor (IP_3Rs) in endoplasmic reticulum (ER) membranes and cellular transient receptor potential vanilloid (TRPV) 4 channels.[24–26] Consequently, disease-induced or pharmacological perturbations of these signaling pathways may greatly affect CBF responses to neuronal activity.[24,27]

Notably, it has been shown that Ang II modulates Ca^{2+} levels in cultured rat astrocytes through triggering AT1 receptor-dependent Ca^{2+} elevations, which is associated with both Ca^{2+} influx and internal Ca^{2+} mobilization.[28,29] However, this effect has not been reported in mice astrocytes, either in vivo or ex vivo. We hypothesized that Ang II locally reduces the vascular response to neuronal stimulations by amplifying astrocytic Ca^{2+} influx and/or intracellular Ca^{2+} mobilization. Using approaches including in vivo laser Doppler flowmetry and in vitro 2-photon fluorescence microscopy on acute brain slices, we tackle this question from local vascular network in vivo to molecular Ca^{2+} signaling pathway in astrocytic endfeet.

In the present study, we provide functional evidence that Ang II impairs the CBF response to the metabotropic glutamate receptor (mGluR) pathway activation in vivo. We also demonstrate that Ang II elevates resting Ca^{2+} levels and the mGluR-dependent Ca^{2+} increases in astrocytic endfeet, and this effect is associated with a switch of the vascular response from dilation to constriction. This effect is reversed by an Ang II AT1 receptor antagonist and a Ca^{2+} chelator. Finally, our results indicate that Ang II potentiates Ca^{2+} elevation through intracellular Ca^{2+} mobilization and TRPV4-mediated Ca^{2+} influx during NVC. These observations may unveil the possible mechanisms by which hypertension impairs NVC.

METHODS

This article adheres to the Transparency and Openness Promotion (TOP) Guidelines, and Institutional Review Board approval was obtained. The data that support the findings of this study are available from the corresponding author upon reasonable request.

Mice

Male C57BL/6 mice 8 to 12 weeks old (Charles River, St-Constant, Canada) were housed individually in a

temperature-controlled room with ad libitum access to water and a standard protein rodent diet (Envigo #2018 Teklad global 18% protein rodent diet). The study was approved by the Committee on Ethics of Animal Experiments of the Université de Montréal in accordance with the principles outlined by the Canadian Council on Animal Care and by the ARRIVE (Animal Research: Reporting of In Vivo Experiments) guidelines. Given that, at this age, female mice are protected from the deleterious effects of Ang II on cerebrovascular functions,[30] only male mice were used.

CBF Monitoring

CBF in the somatosensory cortex was monitored using laser Doppler flowmetry as described before.[18] Briefly, mice were anesthetized with isoflurane (maintenance, 2%) in oxygen and artificially ventilated through a tracheotomy. A femoral artery was cannulated for recording mean arterial pressure and collecting blood samples to analyze pH and blood gases. The trachea was intubated and mice were artificially ventilated (Harvard Apparatus, Canada) with an oxygen–nitrogen mixture adjusted to provide an arterial P_{O_2} of 120 to 140 mm Hg and P_{CO_2} of 33 to 38 mm Hg. Rectal temperature was maintained at 37 °C using a thermostatically controlled heating device (Harvard Apparatus, Canada). After surgery, anesthesia was maintained with urethane (750 mg/kg, ip) and α-chloralose (50 mg/kg, ip). A 2×2-mm craniotomy was performed to expose the somatosensory cortex and the dura was removed. Artificial cerebrospinal fluid (aCSF) (35–36 °C; pH 7.3–7.4) was continuously superfused over the somatosensory cortex where CBF was monitored using a Doppler laser probe (ADInstruments, Colorado Springs, CO, USA) connected to a computerized data acquisition system (Powerlab with Labchart Pro; AD Instruments, Colorado Springs, CO, USA). CBF was expressed as percentage increase relative to resting level.

Experimental Protocol for CBF Measurement

The exposed cortex was continuously superfused with aCSF and all drugs were dissolved in this buffer. To study the increase in CBF produced by neuronal activity, the somatosensory cortex was activated by gently stroking the contralateral whiskers at a frequency of 4 Hz for 60 seconds in triplicate, with a resting period of 3 minutes. Five-minute perfusions with the mGluR agonist 1S, 3R-1-aminocyclopentane-*trans*-1,3-dicarboxylic acid (t-ACPD) (25 µmol/L) were performed with or without the sodium channel blocker tetrodotoxin (3 µmol/L; topical superfusion; Alomone labs, Israel), used to block neuronal activity. Responses to whisker stimulations (5 mice/group) or *t*-ACPD (6 mice/group) were compared before and after a 30-minute superfusion with Ang II (50 nmol/L) or its vehicle (aCSF). In another group of mice, the mGluR5 antagonist, 2-methyl-6-(phenylethynyl) pyridine hydrochloride (30 µmol/L), with or without the mGluR1 antagonist, (S)-(+)-alpha-amino-4-carboxy-2-methylbenzene-acetic acid (LY367385, 500 µmol/L), were superfused over the somatosensory cortex during 20 minutes before assessing the vascular responses to whisker stimulations.

Brain Slice Preparation

Mice were euthanized with an overdose of isoflurane and immediately decapitated. Their brain was quickly removed and placed into 4 °C aCSF (125 mmol/L NaCl, 3 mmol/L KCl, 26 mmol/L $NaHCO_3$, 1.25 mmol/L NaH_2PO_4, 2 mmol/L $CaCl_2$, 1 mmol/L $MgCl_2$, 4 mmol/L glucose, and 400 µmol/L L-ascorbic acid) equilibrated at a pH of 7.4 with a 95% O_2/5% CO_2 gas mixture. Coronal slices (175-µm thick) were cut at the level of the somatosensory cortex using a vibratome (VT1000S; Leica, Wetzlar, Germany) and stored in the previous solution at room temperature before loading dye or caged Ca^{2+} compound.

Brain Slices Imaging of Ca^{2+} and Arteriolar Diameter

Brain slices were incubated at 28 °C under constant agitation for 1 hour in oxygenated aCSF, the Ca^{2+} indicator Fluo-4 AM (10 µmol/L; Invitrogen, Burlington, Canada), Cremophor EL (0.005% [vol/vol]; Sigma, Oakville, Canada), and pluronic acid F-127 (0.025% [wt/vol]; EMD Calbiochem, Gibbstown, NJ, USA). In some experiments, slices were coloaded with the caged Ca^{2+} compound, 1-[4,5 dimethoxy-2-nitrophenyl]-EDTA-AM (10 µmol/L; Interchim, France) or the Ca^{2+} chelator 1,2-Bis(2-aminophenoxy)ethane-*N,N,N',N'*-tetra-acetic acid tetrakis (acetoxymethyl ester) (BAPTA-AM; 1 µmol/L; Sigma-Aldrich, ON, Canada) for 60 minutes using the same loading conditions. The dose of BAPTA-AM was determined from a dose–response curve in order to get a Ca^{2+} increase in response to *t*-ACPD in the presence of Ang II comparable to the increase in the presence of the vehicle. Under these conditions, compounds attached to AM esters preferentially load into astrocytes as we verified with the specific astrocyte marker sulforhodamine 101 at the end of each experiment. After incubation, slices were transferred into aCSF at room temperature.

Imaging was performed with a multiphoton laser scanning upright microscope (BX61WI; Olympus, Tokyo, Japan) coupled to a Ti:Sapphire laser (MaiTai HP DeepSee; Spectra Physics, Santa Clara, CA, USA) and equipped with a 40× water immersion objective (digital zoom factor of 3.5). Time-lapse images were acquired using the FV10-ASW software (version 3.0; Olympus, Tokyo, Japan) and displayed the arteriole diameter/

morphology as visualized by infrared differential interference contrast imaging, simultaneously with the free intracellular Ca^{2+} (Fluo-4 AM) in astrocyte endfeet. Fluo-4 AM was excited at 805 nm by the Ti:sapphire laser (100-fs pulses, 0.5 W) and fluorescence emission was collected using a 575/150-nm bandpass filter. For Ca^{2+} uncaging experiments, a 2.5×2.5 µm region of interest within an endfoot (zoomed for the duration of 1 frame) was scanned at a laser intensity ≈6× higher than that used for imaging. In uncaging experiments, the laser was set at 730 nm, which allows simultaneous excitation of Fluo-4 and photolysis of the caged Ca^{2+}, 1-[4,5 dimethoxy-2-nitrophenyl]-EDTA.[18] Reproducible increases in $[Ca^{2+}]i$ were detected over multiple uncaging events, and no increase in $[Ca^{2+}]i$ was detected in nonloaded slices. The laser power used for Ca^{2+} imaging was below the threshold for Ca^{2+} uncaging. Matched time controls were also performed. Infrared differential interference contrast allowed the evaluation of brain slice integrity through the visualization of dead neurons, which was an exclusion criterion.

For every experiment, a descending arteriole branching from a pial artery was selected in the somatosensory cortex layers 2 to 5. Only arterioles located 50 to 100 µm below the cut surface of brain slices were selected. Morphological criteria were used to distinguish arterioles from venules and capillaries as described earlier.[18] An astrocyte endfoot adjacent to the arteriole was then selected at the same focal plane displaying the largest lumen diameter of arterioles and the highest Fluo-4 fluorescence of endfoot. Images were processed with Image J software (v.1.45r for Mac OS; The National Institutes of Health, Bethesda, MD, USA) and the arteriole luminal diameter was measured adjacently to the selected endfoot on each image. The distance between 2 points was calculated from a line perpendicular to the arterial walls. The baseline diameter was obtained from the average of 20 successive images preceding stimulation.

Experimental Protocol for Brain Slice Studies

Before each experiment, a slice was transferred to the imaging chamber, secured with a slice anchor, and constantly perfused with 35 °C oxygenated (5% CO_2/95% O_2, pH ≈7.4; oxygen level ≈35% as measured in the slice chamber) aCSF at a speed of 2 mL/min. The first stimulation was performed after 20 minutes incubation with the thromboxane-A_2 receptor agonist, U46619 (Cayman Chemicals, 150 nmol/L; Ann Arbor, MI, USA). This concentration of U46619 pre-constricts the vessels to a tone that allows both vasodilation and vasoconstriction, thus mimicking the physiological vascular tone (≈20%–30% of the unconstricted baseline diameter). The stimulations with the mGluR agonist, *t*-ACPD (50 µmol/L; 3 minutes; Tocris Bioscience, Bristol, UK), were assessed before and after 20 minutes perfusion with vehicle (aCSF and U46619) or with the same solution containing 100 nmol/L of Ang II. In another group of slices, Ca^{2+} was uncaged in astrocytes after a resting period of 20 minutes in the presence of the vehicle or with the same solution containing 100 nmol/L of Ang II. The concentration of Ang II was determined from different doses (results not shown), which indicated that 100 nmol/L corresponds to a concentration that is low enough to not change the resting vascular diameter but high enough to provide reproducible data. Candesartan (10 µmol/L), HC067047 (10 µmol/L), cyclopiazonic acid (30 µmol/L), and xestospongin C (XC; 10 µmol/L) were added to the medium 5 minutes before the perfusion of Ang II.

Endfoot Ca^{2+} Analysis

Astrocyte endfoot Ca^{2+} concentrations were determined using the maximal fluorescence method as described earlier.[18] To summarize, ionomycin (407950, 10 µmol/L; EMD Calbiochem, Gibbstown, NJ, USA) and 20 mmol/L Ca^{2+} were immediately added to aCSF at the end of experiment to obtain the maximal fluorescence. The maximal fluorescence value was measured within a region of interest (15 pixels×15 pixels, or 1.8×1.8 µm) in the selected endfoot. Using this value and experimental parameters, the estimated $[Ca^{2+}]i$ was calculated using Maravall's formula.[18,31] Fractional fluorescence (F1/F0) values reflect the fluorescence intensity for a region of interest in each image (F1) divided by a mean fluorescence value (F0) taken from 20 images before stimulation.

Statistical Analysis

Data were analyzed with GraphPad Prism v7.0 (La Jolla, USA). All results are presented as raw data ±SD. Multiple comparisons were performed by 1-way ANOVA, 2-way ANOVA, or 2-way ANOVA repeated measures as appropriate with the Bonferroni post hoc test to compare differences among groups. The 2-tailed unpaired Student *t* test was performed for comparison between 2 groups. Differences at $P \leq 0.05$ were considered statistically significant. The statistical test and the number of animals are specified in the figure legends.

RESULTS

Ang II Attenuates CBF Responses to Whisker Stimulation and mGluR Activation

The effect of Ang II on CBF responses to whisker stimulation and the mGluR agonist, *t*-ACPD, was investigated. We confirmed that Ang II attenuated

whisker stimulation-induced CBF increase (Vehicle: 18.5% ± 1.2%; Ang II: 11.3% ± 1.9%, ***P*<0.01, Figure 1A and 1C, n=5–6) without changing resting baseline (Figure 1B), and discovered that Ang II markedly reduced the CBF response to *t*-ACPD from 18.5% ± 4.5% to 11.7% ± 2.3% (***P*<0.01; Figure 1A and 1C, n=4–6). Notably, even in the presence of tetrodotoxin (3 µmol/L), *t*-ACPD increases CBF at the same level as without tetrodotoxin and Ang II still significantly attenuated *t*-ACPD-induced CBF increase (**P*<0.05, Figure S1A, n=4–6), suggesting that these effects are independent of neuronal activity. The mGluR5 antagonist, 2-methyl-6-(phenylethynyl) pyridine hydrochloride (30 µmol/L), and mGluR1 antagonist (LY367385; 500 µmol/L) were added during 20 minutes to further verify the involvement of these specific mGluR in NVC (whisker stimulation). Although LY367385 had no additive effect on NVC, 2-methyl-6-(phenylethynyl) pyridine hydrochloride did inhibit the CBF response to whisker stimulation by 55% (**P*<0.05; Figure S1B, n=2).

Ex Vivo Ang II Promotes Vasoconstriction Over Vasodilation in Response to mGluR Activation

Time-control experiments showed that 20 minutes incubation with the vehicle, aCSF, did not change the vascular response to *t*-ACPD (difference of 0.5 ± 1.8% between the responses to *t*-ACPD before [resting] and after 20 minutes with the vehicle, Figure 2A, n=3–4). Indeed, in the control group (vehicle), parenchymal arterioles dilate in response to *t*-ACPD by 9.6% ± 1.2% (Figure 2B and 2C, upper panel). However, 20 minutes incubation with Ang II (100 nmol/L) significantly reversed the polarity of the vascular response to *t*-ACPD, inducing vasoconstriction instead of vasodilation

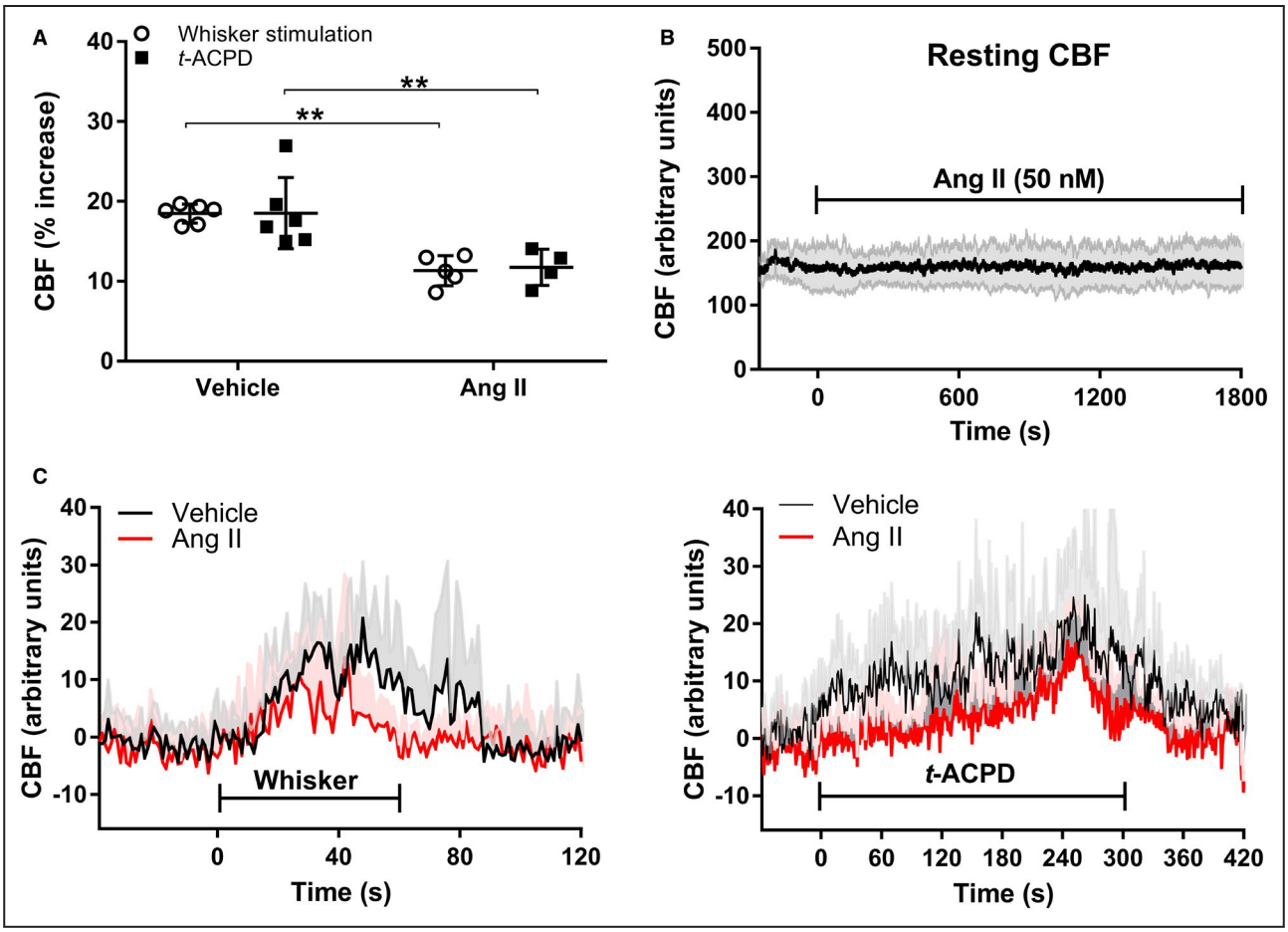

Figure 1. Ang II attenuates CBF responses to whisker stimulation and mGluR activation in the somatosensory cortex.
A, Thirty-minute perfusion with Ang II (50 nmol/L) attenuates CBF increases in response to whisker stimulations (n=5–6) and to the mGluR agonist, *t*-ACPD (5 minutes, 25 µmol/L; n=4–6). **B**, Traces of averaged resting CBF acquired before and during Ang II (50 nmol/L) superfusion. **C**, Traces of averaged CBF responses induced by whisker stimulation (left panel) or *t*-ACPD (right panel) superfusion in the presence or absence of Ang II were acquired at 1 Hz using laser Doppler flowmetry. SD is represented by the lighter tone shade surrounding each curve. (***P*<0.01; 2-way ANOVA followed by Bonferroni correction). Ang II indicates angiotensin II; CBF, cerebral blood flow; mGluR, metabotropic glutamate receptor; SD, standard deviation; and *t*-ACPD, 1S, 3R-1-aminocyclopentane-*trans*-1,3-dicarboxylic acid1S.

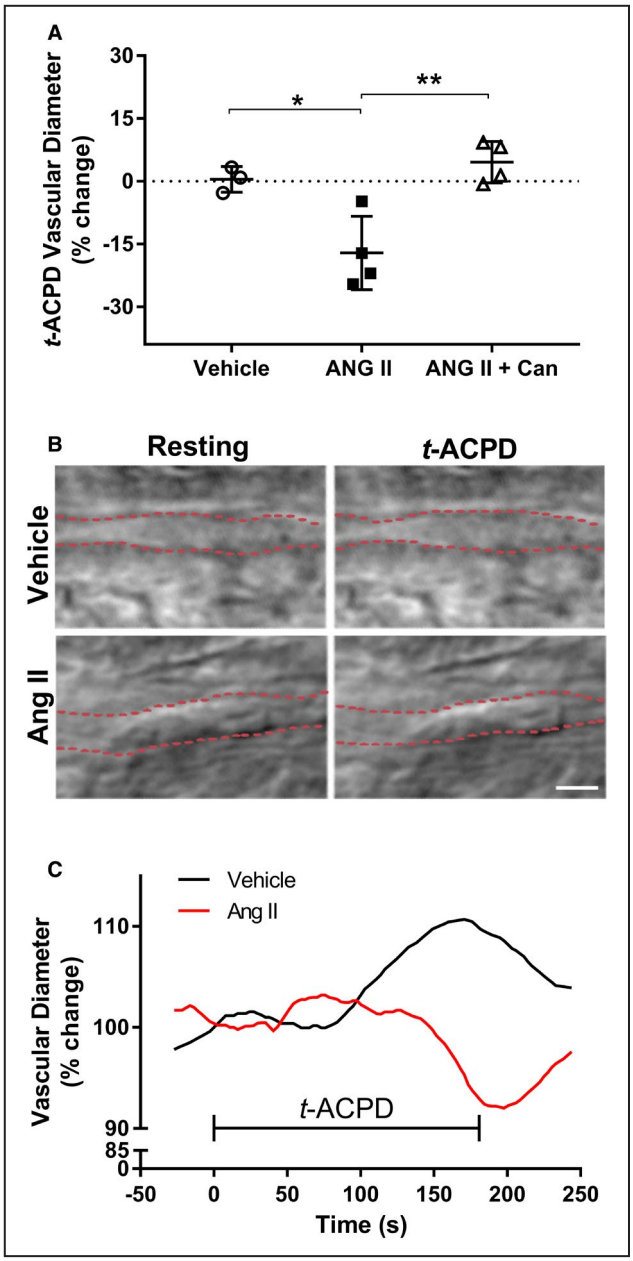

Figure 2. Ang II promotes constriction over dilation of the somatosensory cortex parenchymal arteries in response to *t*-ACPD in acute brain slices.

A, Differences expressed in percent change between the vascular responses to *t*-ACPD (50 µmol/L) before (resting) and after 20 minutes of incubation with the vehicle (artificial cerebrospinal fluid), Ang II (100 nmol/L), or Ang II in the presence of the AT1 antagonist, candesartan (10 µmol/L). Candesartan was added 5 minutes before Ang II. **B**, Representative pictures of resting vascular state and maximum vascular response to *t*-ACPD after 20 minutes of incubation with the vehicle or Ang II. Images are obtained from infrared differential interference contrast infrared differential interference contrast imaging. The lumen of parenchymal arteries is outlined by red lines. The diameter was calculated from the average of 20 successive images at resting state and maximum vascular response to *t*-ACPD (scale bar=20 µm). **C**, Time-course traces of luminal diameter changes in response to *t*-ACPD after 20 minutes of incubation with the vehicle (black line) or Ang II (red line). Vasodilatation to *t*-ACPD in the presence of the vehicle is converted into vasoconstriction after 20 minutes incubation with Ang II. (*P<0.05, **P<0.01; 1-way ANOVA followed by Bonferroni correction; n=3–4). Ang II indicates angiotensin II; Can, candesartan; and *t*-ACPD, 1S, 3R-1-aminocyclopentane-*trans*-1,3-dicarboxylic acid.

(difference of –17.2 ± 8.7 between the responses to *t*-ACPD before and after Ang II *P<0.05; Figure 2A, 2B and 2C lower panel; n=3–4). This effect was blocked by the angiotensin receptor antagonist, candesartan (**P<0.01, Figure 2A, n=3–4), indicating that AT1 receptors contribute to the effect of Ang II on the *t*-ACPD-induced vascular response. Neither Ang II nor candesartan changed the resting vascular diameter and candesartan alone did not modify the vascular response to *t*-ACPD (data not shown).

Ang II Increases Basal and *t*-ACPD-Induced $[Ca^{2+}]_i$ Rise in Astrocytic Endfeet

To determine whether the effect of Ang II on mGluR-dependent vascular responses is determined by Ca^{2+} increases in astrocytic endfeet, Ca^{2+} fluorescence in an astrocytic endfoot abutting an arteriole was imaged. The amplitude of Ca^{2+} response to mGluR activation by *t*-ACPD in astrocyte endfeet was markedly potentiated after 20 minutes exposition to Ang II (100 nmol/L) compared with the vehicle (**P<0.01; Figure 3, n=9–10). Because the Fluo4 signal decreases with time and we wanted to compare the effects of several drugs on Ca^{2+} levels, $[Ca^{2+}]_i$ was then estimated using the Maravall's formula.[18,31] Thus, after 20 minutes incubation with Ang II, the average resting $[Ca^{2+}]_i$ in the astrocytic endfeet was nearly twice the level found in the vehicle group (*P<0.05; Figure 4A and 4B, n=4–5). The resting spontaneous $[Ca^{2+}]_i$ oscillations expressed as the coefficient of variation was also increased in the presence of Ang II (*P<0.05, Figure 4D and 4E, n=4). Notably, the maximal $[Ca^{2+}]_i$ increase in response to *t*-ACPD in the presence of Ang II was 3 times higher compared with the vehicle group (*P<0.05, Figure 4A and 4B, n=4–5). The AT1 receptor blocker (angiotensin receptor antagonist), candesartan, markedly reduced the maximal $[Ca^{2+}]_i$ increase induced by *t*-ACPD in the presence of Ang II to a level comparable to the vehicle group (*P<0.05 Figure 4A and 4B, n=4–5). Candesartan alone did not modify the $[Ca^{2+}]_i$ response to *t*-ACPD (data not shown). Consistent with this observation, the AUC showing the total amount of Ca^{2+} during mGluR activation by *t*-ACPD was significantly increased in the presence of Ang II compared with the vehicle group, the effect of which was also prevented by candesartan (***P<0.001 Figure 4C, n=4–5).

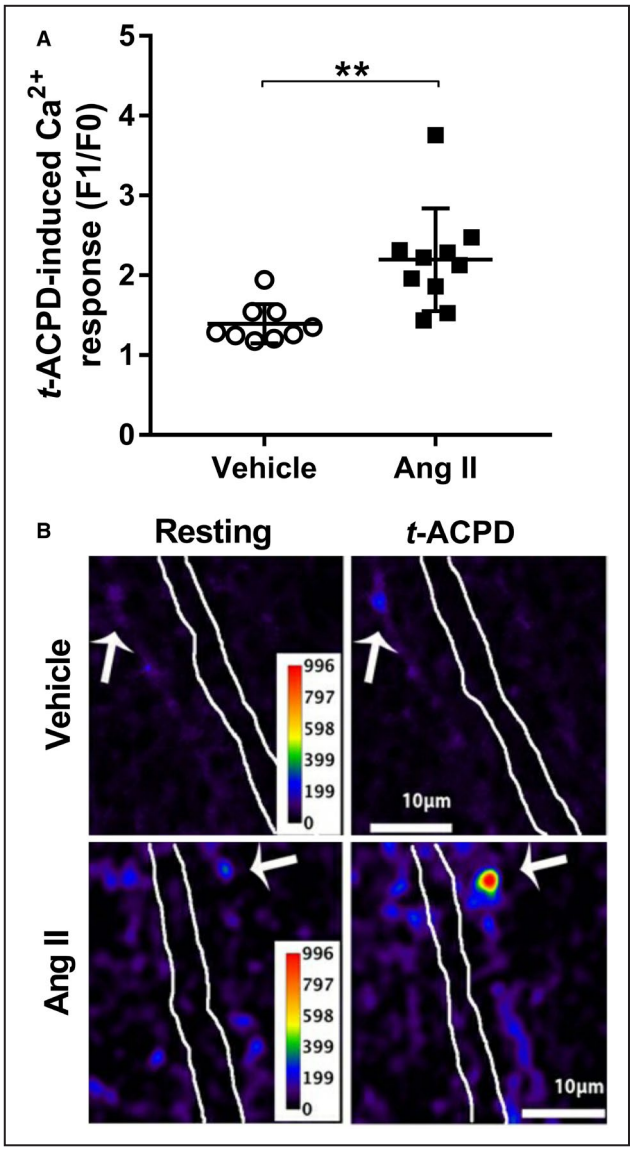

Figure 3. Ang II amplifies Ca^{2+} increases in astrocytic endfeet in response to *t*-ACPD in acute brain slices.
A, Ang II (100 nmol/L) significantly increases the amplitude of astrocytic endfeet Ca^{2+} response to *t*-ACPD (50 µmol/L), measured as fractional fluorescence (F1/F0). **B**, Representative images showing astrocytic endfoot Ca^{2+} increases in response to *t*-ACPD before and after 20 minutes of incubation with Ang II or its vehicle. $[Ca^{2+}]_i$ in astrocytic endfeet surrounding a parenchymal arteriole in brain slice is pseudocolor-mapped (based on fluo-4 fluorescence) (Pseudocolors legend unit corresponds to nmol/L of Ca^{2+}; scale bar=10 µm). The white arrows show Ca^{2+} spots in analyzed astrocytic endfeet. The lumen of the artery is outlined by white lines. (**P<0.01; 2-tailed unpaired *t* test; n=9–10). Ang II indicates angiotensin II; and *t*-ACPD, 1S, 3R-1-aminocyclopentane-*trans*-1,3-dicarboxylic acid.

Elevated Endfoot $[Ca^{2+}]_i$ Results in Attenuated Vascular Responses in the Presence of Ang II

To bypass the mGluR-associated pathway and directly detect the effect of Ang II on the vascular response in conditions of similar $[Ca^{2+}]_i$ increases, 2-photon photolysis of caged Ca^{2+} in the specific endfoot was performed in the same group of brain slices. Upon similar $[Ca^{2+}]_i$ increases compared with the vehicle group (Figure 5C), Ang II did not promote vasoconstriction (Figure 5A, 5B, and 5D, n=5–7).
Then, the levels of endfeet $[Ca^{2+}]_i$ in the presence of Ang II were normalized following a pre-incubation of the Ca^{2+} chelator (BAPTA-AM, 1 µmol/L for 1 hour). In these conditions, parenchymal arterioles dilated in response to *t*-ACPD in the presence of Ang II (*P<0.05; Figure 5E through 5F, n=–7).

IP_3Rs and TRPV4 Channels Mediate Ang II Action on Endfoot Ca^{2+} Signaling

To investigate the underlying mechanism by which Ang II amplifies endfoot $[Ca^{2+}]_i$ increase, we first used the sarcoplasmic reticulum/ER Ca^{2+} ATPase (SERCA) inhibitor, cyclopiazonic acid (30 µmol/L), to deplete ER Ca^{2+} stores. After 20 minutes incubation with cyclopiazonic acid, the *t*-ACPD-induced increases of $[Ca^{2+}]_i$ in the absence or presence of Ang II were significantly reduced from 1.35 ± 0.16 to 1.16 ± 0.03 (*P<0.05, Figure 6A, n=5–6) and from 2.02 ± 0.43 to 1.27 ± 0.14 (**P<0.01, Figure 6B; n=4–6), respectively, without changing the resting Ca^{2+} level (Figure S2; n=3–6). To validate the results and further explore sources of the internal Ca^{2+} mobilization, we applied XC (10 µmol/L), an IP_3Rs inhibitor that partially inhibits IP_3Rs in brain slices.[24] Although Ca^{2+} increase induced by *t*-ACPD was not affected by XC (Figure 6A; n=5–6), it did significantly reduce the maximal ratio of increased Ca^{2+} induced by *t*-ACPD in the presence of Ang II from 2.02 ± 0.43 to 1.37 ± 0.10 (*P<0.01; Figure 6B; n=4–6). We also tested the effect of Ang II on endfoot $[Ca^{2+}]_i$ in the presence of the TRPV4 antagonist, HC067047 (10 µmol/L). HC067047 inhibited the effect of Ang II on $[Ca^{2+}]_i$ increases in response to *t*-ACPD (*P<0.05, Ang II: 447.3 ± 66.3 nmol/L, Ang II+HC067047: 292.8 ± 118.2 nmol/L, Figure 6D; n=6–8) without changing the resting $[Ca^{2+}]_i$ or the $[Ca^{2+}]_i$ response to *t*-ACPD in the absence of the peptide (Figure 6C).

DISCUSSION

We investigated the mechanisms by which Ang II, a hormone involved in the initiation and maintenance of hypertension, alters NVC, and thus brain imaging signals evoked by neuronal activation. Previous studies have clearly shown that the effects of Ang II on NVC are independent of blood pressure[4,11,12] and that oxidative stress and inflammation are involved.[8,10,16,32] However, little has been done to investigate the effects of Ang II on the signaling of the cells that constitute the neurovascular unit. A recent study demonstrated

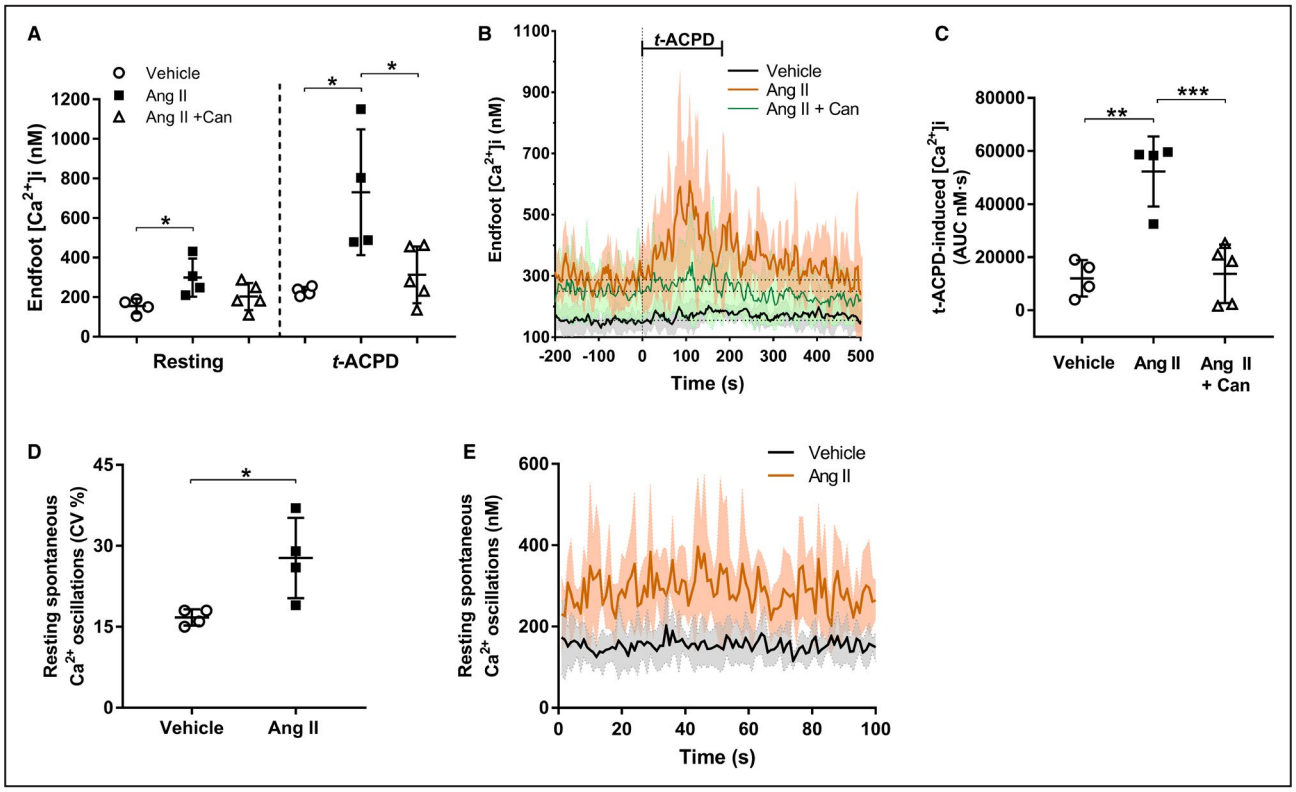

Figure 4. In acute brain slices, Ang II increases resting $[Ca^{2+}]_i$ and *t*-ACPD-induced Ca^{2+} rises in astrocytic endfeet.
A, Estimated $[Ca^{2+}]_i$ from the fluo-4 signal and calculated using Maravall's formula at resting state and in response to *t*-ACPD (50 µmol/L) in astrocytic endfeet incubated with the vehicle, Ang II (100 nmol/L), or Ang II+candesartan (Can, 10 µmol/L). Can was added 5 minutes before Ang II incubation (n=4–5). **B**, Average of the estimated Ca^{2+} levels of all experiments for each time point in response to *t*-ACPD, suggesting a potentiated response in the Ang II group as compared with the vehicle and the Ang II+Can groups. SD is shown by the lighter tone shade surrounding each curve. **C**, AUC of Ca^{2+} increases in response to *t*-ACPD after 20 minutes of incubation with vehicle, Ang II, or Ang II+Can (n=4–5). **D**, The CV in percentage of the resting spontaneous Ca^{2+} oscillations in the presence of the vehicle or Ang II in cortical astrocytes (n=4). **E**, Traces of averaged resting $[Ca^{2+}]_i$ acquired in the presence of the vehicle or Ang II in cortical astrocytes. Shaded areas represent SD (**P*<0.05, ***P*<0.01, ****P*<0.001; 1-way ANOVA followed by Bonferroni correction for multiple comparisons or 2-tailed unpaired *t* test for the comparison between 2 groups). Ang II indicates angiotensin II; CV, coefficient of variation; SD, standard deviation and *t*-ACPD, 1S, 3R-1-aminocyclopentane-*trans*-1,3-dicarboxylic acid.

that chronic Ang II exposure alters astrocytic Ca^{2+} responses.[33] However, it was not clear in that study whether Ang II mediated these effects through chronic actions on the neurovascular unit structure or through specific effects on signaling pathways. Using in vivo and ex vivo local application of Ang II on the somatosensory cortex, we found that (1) Ang II increases resting astrocytic endfoot $[Ca^{2+}]_i$ and in response to mGluR activation; (2) IP_3Rs and TRPV4 channels mediate Ang II action on astrocytic Ca^{2+} signaling; (3) Ang II attenuates CBF elevation induced by mGluR activation; (4) ex vivo, Ang II promotes vasoconstriction over vasodilation in response to mGluR activation, an effect dependent on astrocytic Ca^{2+} levels; and (5) both effects of Ang II on vascular and astrocytic Ca^{2+} responses following mGluR stimulation are dependent on its AT1 receptor.

These findings represent the first indication that locally produced Ang II could impair NVC through its action on astrocytic regulation of vascular tone. Previous studies have reported that intravenous injection or topical application of Ang II over the somatosensory cortex attenuates whisker stimulation–induced CBF increase, thus mimicking the circulating or local parenchymal effects of Ang II.[4,10] This Ang II effect does not impair neuronal field potentials,[4] suggesting that Ang II interferes with the mediators responsible for the increases in CBF evoked by neuronal activity instead of neuronal activity itself.[4] Our present experimental conditions show the local parenchymal effects of Ang II. This aspect is of considerable importance since age-associated brain dysfunctions or neurodegenerative diseases are improved by angiotensin receptor antagonists that cross the blood–brain barrier,[34] suggesting a role of local parenchymal Ang II in these pathologies. We found that topical perfusion of Ang II attenuates CBF increases in response to whisker stimulations or mGluR activation at a concentration that does not decrease resting CBF. In ex vivo experiment, Ang II promotes vasoconstriction over vasodilation in response

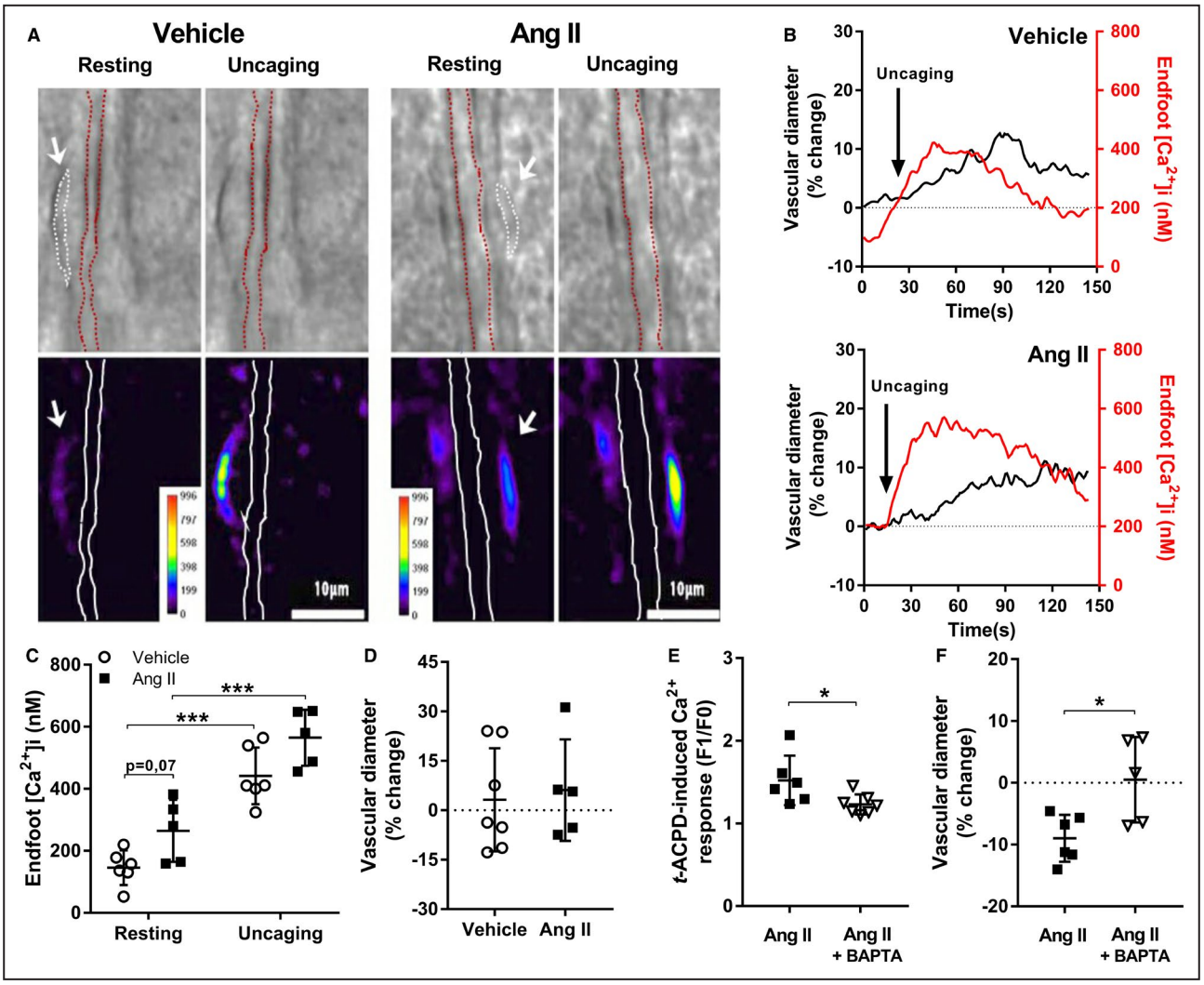

Figure 5. Ang II does not modulate the vascular response to Ca^{2+} increases controlled by photolysis or Ca^{2+} chelation in acute brain slices.

A, Example of simultaneous recording of changes in arteriolar diameter (upper panels) and astrocytic endfoot Ca^{2+} increases (lower panels) before (resting) and after 2-photon Ca^{2+} uncaging (excitation volume <3 µm^3) for ≈0.5 s in acute brain slices incubated with Ang II (100 nmol/L) or its vehicle. Upper panels: Images of parenchymal arteries obtained from infrared differential interference contrast imaging. Lower panels: Pseudocolor-mapped $[Ca^{2+}]_i$ (based on fluo-4 fluorescence) representing $[Ca^{2+}]_i$ in astrocytic endfeet surrounding a parenchymal arteriole in acute brain slice (Pseudocolors legend unit corresponds to nmol/L of Ca^{2+}; scale bar=10 µm). Dashed white lines in the upper panels and arrows in the lower panels show an astrocyte endfoot abutting a parenchymal arteriole in acute brain slice loaded with the caged Ca^{2+}, DMNP-EDTA (10 µmol/L, 1 h). The lumen of parenchymal arteries is outlined by red lines in the upper panels and white lines in the lower panels. **B**, Time course traces of changes in endfoot Ca^{2+} (red) and arteriole diameter (black) after Ca^{2+} uncaging in the presence of Ang II (lower panel) or its vehicle (upper panel). **C**, Astrocytic Ca^{2+} levels before (resting) and at its peak after Ca^{2+} uncaging in the same group of brain slices in the presence of Ang II or its vehicle (n=5–7; ***P<0.001; 2-way ANOVA repeated measures followed by Bonferroni correction for multiple comparisons). **D**, The percentage of diameter changes in response to Ca^{2+} uncaging in the presence of Ang II or its vehicle (n=5–7). **E**, Astrocytic endfeet Ca^{2+} increases in response to *t*-ACPD, measured as F1/F0 and (**F**) arteriolar diameter changes in acute brain slices perfused with Ang II alone or with the Ca^{2+} chelator, BAPTA-AM (n=5–7). (**E** and **F;** *P<0.05, 2-tailed unpaired *t* test for the comparison between 2 groups). Ang II indicates angiotensin II; BAPTA-AM, 1,2-Bis(2-aminophenoxy)ethane-*N,N,N',N'*-tetra-acetic acid tetrakis (acetoxymethyl ester); DMNP-EDTA, 1-[4,5 dimethoxy-2-nitrophenyl]-EDTA-AM; and *t*-ACPD, 1S, 3R-1-aminocyclopentane-*trans*-1,3-dicarboxylic acid.

to mGluR activation at a concentration previously reported not affecting neuronal excitability or eliciting a vasoconstriction at resting state (≤100 nmol/L).[16] Our observed effects are specific to the astrocytes for the following reasons: (1) a contribution of the parenchymal smooth muscles is unlikely since smooth muscles of arteries of the somatosensory cortex do not contain AT1 receptors[23]; (2) for uncaging experiments, we were very careful not to uncage in an astrocyte that overlaps smooth muscle cells; (3) it is also unlikely that AM

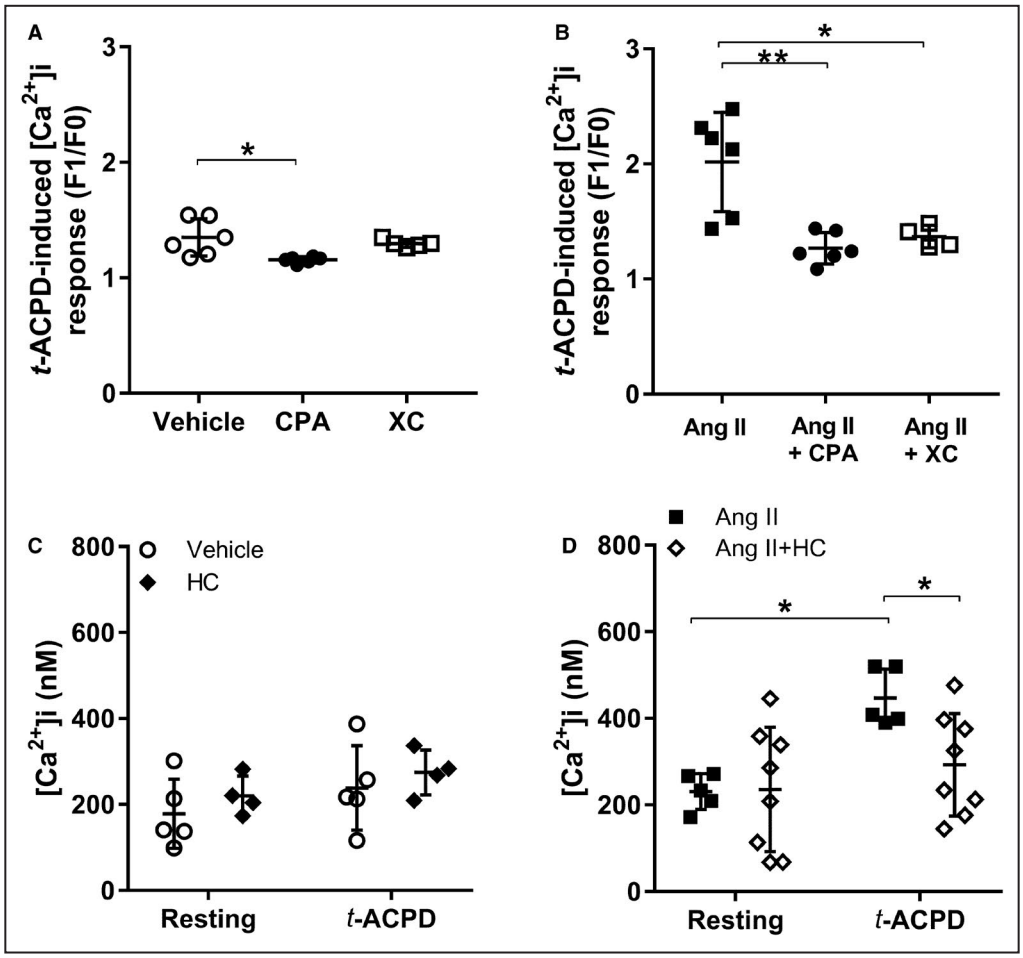

Figure 6. IP_3Rs and TRPV4 channels mediate Ang II action on astrocytic endfoot Ca^{2+} levels in acute brain slices.

A, Astrocytic endfeet Ca^{2+} increases in response to *t*-ACPD, measured as F1/F0 in brain slices perfused with vehicle or in the presence of the sarcoplasmic reticulum (SR)/ER Ca^{2+} ATPase (SERCA) inhibitor, CPA (30 µmol/L) or the partial IP_3Rs inhibitor, XC (10 µmol/L; n=5–6). **B**, Astrocytic endfeet Ca^{2+} increases in response to *t*-ACPD, measured as F1/F0 in brain slices perfused with Ang II (100 nmol/L) alone or in the presence of CPA 30 µmol/L or XC 10 µmol/L (n=4–6). **C**, Estimated $[Ca^{2+}]_i$ at resting state and in response to *t*-ACPD in astrocytic endfeet with the vehicle or HC (10 µmol/L; n=4–5). **D**, Estimated $[Ca^{2+}]_i$ at resting state and in response to *t*-ACPD in astrocytic endfeet in the presence of Ang II (50 nmol/L) or with HC 10 µmol/L (n=5–8) in different groups of brain slices. (**P*<0.05, ***P*<0.01; **A** through **B**, 1-way ANOVA followed by a Bonferroni correction for multiple comparisons; **D**, 2-way ANOVA followed by Bonferroni correction for multiple comparisons). Ang II indicates angiotensin II; CPA, cyclopiazonic acid; HC, HC067047; IP3Rs, inositol 1,4,5-trisphosphate receptor; *t*-ACPD, 1S, 3R-1-aminocyclopentane-*trans*-1,3-dicarboxylic acid; TRPV4, transient receptor potential vanilloid 4; and XC, xestospongin C.

esters penetrate vascular cells since there is no indication of loading vascular cells with AM dyes under our conditions and no effects of BAPTA-AM on vascular diameter had been demonstrated with a loading period of <2 hours[19,35]; (4), the specific astrocytic marker, sulforhodamine 101, was added at the end of each experiment to identify astrocytes. Overall, these results support a growing body of evidence that Ang II can exert detrimental effects on NVC through its local parenchymal action on signaling pathways downstream of the mGluR but independently of neuronal activity or a direct effect of Ang II on smooth muscle cells.

Along with impaired vascular response, Ang II potentiates resting $[Ca^{2+}]_i$, the amplitude of spontaneous Ca^{2+} oscillations, and the Ca^{2+} response to activation of mGluR in astrocytic endfoot. Ca^{2+} serves as a second messenger driving astrocytic control over the microvasculature.[18] This is consistent with the presence of AT1 receptors in the perivascular astrocytes of mice.[36] Astrocytic Ca^{2+} elevation had been associated with both vascular dilation and constriction. Four mechanisms have been proposed to explain this controversy.[18,20,37,38] Vasoconstriction had been explained by a lack of vascular tone or preconstriction,[38] a change

in the level of P_{O_2},[37] high concentrations of nitric oxide (NO) as well as levels of Ca^{2+} increase and the ensuing activation of Ca^{2+}-activated K^+ (BK) channels.[18,20] During our experiments, arterioles were preconstricted and the level of P_{O_2} was constant. We observed that Ang II, through its AT1 receptor, potentiates *t*-ACPD–induced $[Ca^{2+}]_i$ increase in astrocytic endfeet and that stimulation reached the turning point concentration of $[Ca^{2+}]_i$ found by Girouard et al.[18] where astrocytic Ca^{2+} increases are associated with constrictions instead of dilations. The Ang II shift of the vascular response polarity to *t*-ACPD in consistency with the endfoot Ca^{2+} elevation suggests that Ang II–induced Ca^{2+} elevation contributes to the impaired NVC.

The role of astrocytic Ca^{2+} levels on vascular responses in the presence of Ang II was demonstrated by the manipulation of endfeet $[Ca^{2+}]_i$ using 2 opposite paradigms: increase with 2 photon photolysis of caged Ca^{2+} or decrease with Ca^{2+} chelation. When $[Ca^{2+}]_i$ increases occur within the range that induces vasodilation,[18] the presence of Ang II no longer affects the vascular response. Results obtained with these 2 paradigms suggest that Ang II promotes vasoconstriction by a mechanism dependent on astrocytic Ca^{2+} release. Candidate pathways that may be involved in the astrocytic Ca^{2+}-induced vasoconstriction are BK channels,[18] cyclo-oxygenase-1/prostaglandin E2 or the CYP hydroxylase/20-HETE pathways.[39,40] There is also a possibility that elevations in astrocytic Ca^{2+} lead to the formation of NO. Indeed, Ca^{2+}/calmodulin increases NO synthase activity and this enzyme has been observed in astrocytes.[41] In acute mammalian retina, high doses of the NO donor (S)-Nitroso-N-acetylpenicillamine blocks light-evoked vasodilation or transforms vasodilation into vasoconstriction.[20] However, additional experiments will be necessary to determine which of these mechanisms is involved in the Ang II-induced release through IP_3Rs expressed in endfeet[26] and whether they could be abolished in IP_3R2-KO mice.[42] Consistently, pharmacological stimulation of astrocytic mGluR by *t*-ACPD initiates an IP_3Rs-mediated Ca^{2+} signaling in WT but not in IP_3R2-KO mice.[43] Thus, we first hypothesized that Ang II potentiated intracellular Ca^{2+} mobilization through an IP_3Rs-dependent Ca^{2+} release from ER-released Ca^{2+} pathway in response to *t*-ACPD. Indeed, depletion of ER Ca^{2+} store attenuated both Ang II-induced potentiation of Ca^{2+} responses to *t*-ACPD and Ca^{2+} response to *t*-ACPD alone. Furthermore, the IP_3Rs inhibitor, XC, which modestly reduced the effect of *t*-ACPD, significantly blocked the potentiating effects of Ang II on Ca^{2+} responses to *t*-ACPD. The modest effect of XC on the *t*-ACPD-induced Ca^{2+} increases is probably because XC, only partially inhibits IP_3Rs at 20 μmol/L in brain slices.[24] However, it provides further evidence that IP_3Rs mediate the effect of Ang II on astrocytic endfoot Ca^{2+} mobilization.

The Ca^{2+}-permeable ion channel, TRPV4, can interact with the Ang II pathway in the regulation of drinking behavior under certain conditions.[44] In addition, TRPV4 channels are localized in astrocytic endfeet and contribute to NVC.[16,17] Thus, as a Ca^{2+}-permeable ion channel, TRPV4 channel may also contribute to the Ang II action on endfoot Ca^{2+} signaling through Ca^{2+} influx. In astrocytic endfoot, Dunn et al. found that TRPV4-mediated extracellular Ca^{2+} entry stimulates IP_3R-mediated Ca^{2+} release, contributing to Ca^{2+} signaling during NVC.[24] We found that the TRPV4 channel, at least in part, mediated the action of Ang II on endfoot Ca^{2+} signaling in our experimental conditions. Interestingly, TRPV4 exacerbated astrocytic Ca^{2+} increases in response to mGluR5 activation have also been observed in the presence of beta amyloid or of immunoglobulin G from patients with sporadic amyotrophic lateral sclerosis. This suggests that TRPV4-induced NVC impairment may contribute to the pathogenesis of Alzheimer disease or sporadic amyotrophic lateral sclerosis.[45–47] The underlying mechanism by which Ang II potentiates activation of the TRPV4 channel may be through the activation of G_q-coupled AT1 receptors, increasing cytosolic diacylglycerol and IP_3 levels. Then, IP_3Rs-mediated $[Ca^{2+}]_i$ increase may activate TRPV4 channel activity[48]; or diacylglycerol may activate the AKAP150-anchored protein kinase Cα. Upon activation, protein kinase Cα can phosphorylate nearby TRPV4 channels, which increases their opening probability.[49,50] It is also possible that Ang II acts on another cell type, which will then release a factor that increases Ca^{2+} in astrocytes.

Our results suggest that 2 potential mechanisms might engage Ang II-induced astrocytic Ca^{2+} elevation through AT1 receptors: IP_3-dependent internal Ca^{2+} mobilization and Ca^{2+} influx from extracellular space by facilitating TRPV4 channel activation.[29] The present study focuses on astrocytic Ca^{2+} signaling, but other mechanisms may be involved in the detrimental effect of Ang II on NVC. Ang II has been reported to induce human astrocyte senescence in culture through the production of reactive oxygen species,[51] which may also induce IP_3-dependent Ca^{2+} transients.[52] In addition, Ang II may attenuate the endothelium-dependent vasodilatation.[53]

In conclusion, Ang II disrupts the vascular response to *t*-ACPD in the somatosensory cortex in vivo as well as in situ. This is associated with a potentiation of the Ca^{2+} increase in the nearby astrocytic endfeet. Indeed, the present study demonstrates that Ang II increases resting Ca^{2+} levels and potentiates the mGluR agonist-induced Ca^{2+} increases in astrocyte endfeet through triggering intracellular Ca^{2+} mobilization and TRPV4-mediated Ca^{2+} influx in the endfeet. Results obtained by manipulating the level of astrocytic Ca^{2+} suggest that Ca^{2+} levels are responsible for the effect of Ang II on the vascular response to the mGluR

pathway activation. Moreover, the effect of Ang II on astrocytic Ca^{2+} and the ensuing vascular response is dependent on the AT1 receptor. Taken together, our study suggests that the strength of astrocytic Ca^{2+} responses play an essential role in Ang II-induced NVC impairment.

Perspectives

Future treatments regulating the aberrant Ca^{2+} response in astrocytes or its consequences (for example, the high increase of extracellular K^+ levels and the subsequent transformation of vasodilation into vasoconstriction) might help to improve NVC in hypertension or brain diseases involving Ang II. In addition, knowing that estradiol modulates astrocytic functions,[54] it would be interesting to investigate whether sexual difference in NVC is related to a sexual dimorphism of the astrocytic reactivity to Ang II.

ARTICLE INFORMATION

Received December 18, 2020; accepted July 9, 2021.

Affiliations

Department of Pharmacology and Physiology, Faculty of Medicine (M.B., L.L., D.V., H.G.); Groupe de Recherche sur le Système Nerveux Central (GRSNC) (M.B., L.L., D.V., H.G.); and Centre interdisciplinaire de recherche sur le cerveau et l'apprentissage (CIRCA) (D.V., H.G.), Université de Montréal, Montréal, Québec, Canada; and Centre de Recherche de l'Institut de Gériatrie de Montréal, Montréal, Québec, Canada (H.G.).

Sources of Funding

This study was supported by the Heart and Stroke Foundation of Canada (HSFC), Fonds de Recherche du Québec-Santé (FRQS), the Canada Foundation for Innovation (CFI), and the Canadian Institutes of Health Research (CIHR). Hélène Girouard was also the holder of a new investigator award from the FRQS and the HSFC.

Disclosures

None.

Supplementary Material

Figures S1–S2

REFERENCES

1. Girouard H, Iadecola C. Neurovascular coupling in the normal brain and in hypertension, stroke, and Alzheimer disease. *J Appl Physiol*. 2006;100:328–335. DOI: 10.1152/japplphysiol.00966.2005.
2. Dunn KM, Nelson MT. Neurovascular signaling in the brain and the pathological consequences of hypertension. *Am J Physiol Heart Circ Physiol*. 2014;306:H1–H14. DOI: 10.1152/ajpheart.00364.2013.
3. Carnevale D, Mascio G, D'Andrea I, Fardella V, Bell RD, Branchi I, Pallante F, Zlokovic B, Yan SS, Lembo G. Hypertension induces brain beta-amyloid accumulation, cognitive impairment, and memory deterioration through activation of receptor for advanced glycation end products in brain vasculature. *Hypertension*. 2012;60:188–197. DOI: 10.1161/HYPERTENSIONAHA.112.195511.
4. Kazama K, Wang G, Frys K, Anrather J, Iadecola C. Angiotensin II attenuates functional hyperemia in the mouse somatosensory cortex. *Am J Physiol Heart Circ Physiol*. 2003;285:H1890–H1899. DOI: 10.1152/ajpheart.00464.2003.
5. Jennings JR, Muldoon MF, Ryan C, Price JC, Greer P, Sutton-Tyrrell K, van der Veen FM, Meltzer CC. Reduced cerebral blood flow response and compensation among patients with untreated hypertension. *Neurology*. 2005;64:1358–1365. DOI: 10.1212/01.WNL.0000158283.28251.3C.
6. Mogi M, Iwanami J, Horiuchi M. Roles of brain angiotensin II in cognitive function and dementia. *Int J Hypertens*. 2012;2012:169649. DOI: 10.1155/2012/169649.
7. Jackson L, Eldahshan W, Fagan S, Ergul A. Within the brain: the renin angiotensin system. *Int J Mol Sci*. 2018;19:876. DOI: 10.3390/ijms19030876.
8. Faraco G, Sugiyama Y, Lane D, Garcia-Bonilla L, Chang H, Santisteban MM, Racchumi G, Murphy M, Van Rooijen N, Anrather J, et al. Perivascular macrophages mediate the neurovascular and cognitive dysfunction associated with hypertension. *J Clin Invest*. 2016;126:4674–4689. DOI: 10.1172/JCI86950.
9. Biancardi VC, Son SJ, Ahmadi S, Filosa JA, Stern JE. Circulating angiotensin II gains access to the hypothalamus and brain stem during hypertension via breakdown of the blood-brain barrier. *Hypertension*. 2014;63:572–579. DOI: 10.1161/HYPERTENSIONAHA.113.01743.
10. Girouard H, Park L, Anrather J, Zhou P, Iadecola C. Cerebrovascular nitrosative stress mediates neurovascular and endothelial dysfunction induced by angiotensin II. *Arterioscler Thromb Vasc Biol*. 2007;27:303–309. DOI: 10.1161/01.ATV.0000253885.41509.25.
11. Capone C, Faraco G, Park L, Cao X, Davisson RL, Iadecola C. The cerebrovascular dysfunction induced by slow pressor doses of angiotensin II precedes the development of hypertension. *Am J Physiol Heart Circ Physiol*. 2011;300:H397–H407. DOI: 10.1152/ajpheart.00679.2010.
12. Iulita MF, Vallerand D, Beauvillier M, Haupert N, A. Ulysse C, Gagné A, Vernoux N, Duchemin S, Boily M, Tremblay M-È, et al. Differential effect of angiotensin II and blood pressure on hippocampal inflammation in mice. *J Neuroinflammation*. 2018;15:62. DOI: 10.1186/s12974-018-1090-z.
13. Saavedra JM. Evidence to consider angiotensin II receptor blockers for the treatment of early Alzheimer's disease. *Cell Mol Neurobiol*. 2016;36:259–279. DOI: 10.1007/s10571-015-0327-y.
14. Danielyan L, Klein R, Hanson LR, Buadze M, Schwab M, Gleiter CH, Frey WH. Protective effects of intranasal losartan in the APP/PS1 transgenic mouse model of Alzheimer disease. *Rejuvenation Res*. 2010;13:195–201. DOI: 10.1089/rej.2009.0944.
15. Tsukuda K, Mogi M, Iwanami J, Min LJ, Sakata A, Jing F, Iwai M, Horiuchi M. Cognitive deficit in amyloid-beta-injected mice was improved by pretreatment with a low dose of telmisartan partly because of peroxisome proliferator-activated receptor-gamma activation. *Hypertension*. 2009;54:782–787. DOI: 10.1161/HYPERTENSIONAHA.109.136879.
16. Kazama K, Anrather J, Zhou P, Girouard H, Frys K, Milner TA, Iadecola C. Angiotensin II impairs neurovascular coupling in neocortex through NADPH oxidase-derived radicals. *Circ Res*. 2004;95:1019–1026. DOI: 10.1161/01.RES.0000148637.85595.c5.
17. Horiuchi M, Mogi M. Role of angiotensin II receptor subtype activation in cognitive function and ischaemic brain damage. *Br J Pharmacol*. 2011;163:1122–1130. DOI: 10.1111/j.1476-5381.2010.01167.x.
18. Girouard H, Bonev AD, Hannah RM, Meredith A, Aldrich RW, Nelson MT. Astrocytic endfoot Ca2+ and BK channels determine both arteriolar dilation and constriction. *Proc Natl Acad Sci USA*. 2010;107:3811–3816. DOI: 10.1073/pnas.0914722107.
19. Mulligan SJ, MacVicar BA. Calcium transients in astrocyte endfeet cause cerebrovascular constrictions. *Nature*. 2004;431:195–199. DOI: 10.1038/nature02827.
20. Metea MR, Newman EA. Glial cells dilate and constrict blood vessels: a mechanism of neurovascular coupling. *J Neurosci*. 2006;26:2862–2870. DOI: 10.1523/JNEUROSCI.4048-05.2006.
21. Filosa G, Bugatti L, Nicolini M. Vesicular-bullous lesion of a finger followed by disseminated eruption. *Ann Dermatol Venereol*. 2004;131:393–395. DOI: 10.1016/s0151-9638(04)93625-3.
22. Gu X, Chen W, Volkow ND, Koretsky AP, Du C, Pan Y. Synchronized astrocytic Ca(2+) responses in neurovascular coupling during somatosensory stimulation and for the resting state. *Cell Rep*. 2018;23:3878–3890. DOI: 10.1016/j.celrep.2018.05.091.
23. Lind BL, Brazhe AR, Jessen SB, Tan FC, Lauritzen MJ. Rapid stimulus-evoked astrocyte Ca2+ elevations and hemodynamic responses in mouse somatosensory cortex in vivo. *Proc Natl Acad Sci USA*. 2013;110:E4678–E4687. DOI: 10.1073/pnas.1310065110.
24. Dunn KM, Hill-Eubanks DC, Liedtke WB, Nelson MT. TRPV4 channels stimulate Ca2+-induced Ca2+ release in astrocytic endfeet and amplify neurovascular coupling responses. *Proc Natl Acad Sci USA*. 2013;110:6157–6162. DOI: 10.1073/pnas.1216514110.

25. Benfenati V, Amiry-Moghaddam M, Caprini M, Mylonakou MN, Rapisarda C, Ottersen OP, Ferroni S. Expression and functional characterization of transient receptor potential vanilloid-related channel 4 (TRPV4) in rat cortical astrocytes. *Neuroscience*. 2007;148:876–892. DOI: 10.1016/j.neuroscience.2007.06.039.
26. Straub SV, Bonev AD, Wilkerson MK, Nelson MT. Dynamic inositol trisphosphate-mediated calcium signals within astrocytic endfeet underlie vasodilation of cerebral arterioles. *J Gen Physiol*. 2006;128:659–669. DOI: 10.1085/jgp.200609650.
27. Pappas AC, Koide M, Wellman GC. Astrocyte Ca2+ signaling drives inversion of neurovascular coupling after subarachnoid hemorrhage. *J Neurosci*. 2015;35:13375–13384. DOI: 10.1523/JNEUROSCI.1551-15.2015.
28. Gebke E, Muller AR, Jurzak M, Gerstberger R. Angiotensin II-induced calcium signalling in neurons and astrocytes of rat circumventricular organs. *Neuroscience*. 1998;85:509–520. DOI: 10.1016/S0306-4522(97)00601-5.
29. Wang D, Martens JR, Posner P, Sumners C, Gelband CH. Angiotensin II regulation of intracellular calcium in astroglia cultured from rat hypothalamus and brainstem. *J Neurochem*. 1996;67:996–1004. DOI: 10.1046/j.1471-4159.1996.67030996.x.
30. Girouard H, Lessard A, Capone C, Milner TA, Iadecola C. The neurovascular dysfunction induced by angiotensin II in the mouse neocortex is sexually dimorphic. *Am J Physiol Heart Circ Physiol*. 2008;294:H156–H163. DOI: 10.1152/ajpheart.01137.2007.
31. Maravall M, Mainen ZF, Sabatini BL, Svoboda K. Estimating intracellular calcium concentrations and buffering without wavelength ratioing. *Biophys J*. 2000;78:2655–2667. DOI: 10.1016/S0006-3495(00)76809-3.
32. Iulita MF, Duchemin S, Vallerand D, Barhoumi T, Alvarez F, Istomine R, Laurent C, Youwakim J, Paradis P, Arbour N, et al. CD4(+) Regulatory T lymphocytes prevent impaired cerebral blood flow in angiotensin II-induced hypertension. *J Am Heart Assoc*. 2019;8:e009372. DOI: 10.1161/JAHA.118.009372.
33. Diaz JR, Kim KJ, Brands MW, Filosa JA. Augmented astrocyte microdomain Ca(2+) dynamics and parenchymal arteriole tone in angiotensin II-infused hypertensive mice. *Glia*. 2019;67:551–565. DOI: 10.1002/glia.23564.
34. Saavedra JM, Angiotensin II. AT(1) receptor blockers as treatments for inflammatory brain disorders. *Clin Sci*. 2012;123:567–590. DOI: 10.1042/CS20120078.
35. Kip SN, Hunter LW, Ren Q, Harris PC, Somlo S, Torres VE, Sieck GC, Qian Q. [Ca2+]i reduction increases cellular proliferation and apoptosis in vascular smooth muscle cells: relevance to the ADPKD phenotype. *Circ Res*. 2005;96:873–880. DOI: 10.1161/01.RES.0000163278.68142.8a.
36. Alliot F, Rutin J, Leenen PJ, Pessac B. Brain parenchyma vessels and the angiotensin system. *Brain Res*. 1999;830:101–112. DOI: 10.1016/S0006-8993(99)01373-6.
37. Gordon GR, Choi HB, Rungta RL, Ellis-Davies GC, MacVicar BA. Brain metabolism dictates the polarity of astrocyte control over arterioles. *Nature*. 2008;456:745–749. DOI: 10.1038/nature07525.
38. Blanco VM, Stern JE, Filosa JA. Tone-dependent vascular responses to astrocyte-derived signals. *Am J Physiol Heart Circ Physiol*. 2008;294:H2855–H2863. DOI: 10.1152/ajpheart.91451.2007.
39. Dabertrand F, Hannah RM, Pearson JM, Hill-Eubanks DC, Brayden JE, Nelson MT. Prostaglandin E2, a postulated astrocyte-derived neurovascular coupling agent, constricts rather than dilates parenchymal arterioles. *J Cereb Blood Flow Metab*. 2013;33:479–482. DOI: 10.1038/jcbfm.2013.9.
40. Imig JD, Simpkins AN, Renic M, Harder DR. Cytochrome P450 eicosanoids and cerebral vascular function. *Expert Rev Mol Med*. 2011;13:e7. DOI: 10.1017/S1462399411001773.
41. Garcia A. Regulation of the nitric oxide/cyclic GMP system in astroglial cells. *Method Find Exp Clin Pharmacol*. 1997;19(suppl A):23-24.
42. Thrane AS, Rangroo Thrane V, Zeppenfeld D, Lou N, Xu Q, Nagelhus EA, Nedergaard M. General anesthesia selectively disrupts astrocyte calcium signaling in the awake mouse cortex. *Proc Natl Acad Sci USA*. 2012;109:18974–18979. DOI: 10.1073/pnas.1209448109.
43. Nizar K, Uhlirova H, Tian P, Saisan PA, Cheng Q, Reznichenko L, Weldy KL, Steed TC, Sridhar VB, MacDonald CL, et al. In vivo stimulus-induced vasodilation occurs without IP3 receptor activation and may precede astrocytic calcium increase. *J Neurosci*. 2013;33:8411–8422. DOI: 10.1523/JNEUROSCI.3285-12.2013.
44. Tsushima H, Mori M. Antidipsogenic effects of a TRPV4 agonist, 4alpha-phorbol 12,13-didecanoate, injected into the cerebroventricle. *Am J Physiol Regul Integr Comp Physiol*. 2006;290:R1736–R1741. DOI: 10.1152/ajpregu.00043.2005.
45. Lim D, Iyer A, Ronco V, Grolla AA, Canonico PL, Aronica E, Genazzani AA. Amyloid beta deregulates astroglial mGluR5-mediated calcium signaling via calcineurin and Nf-kB. *Glia*. 2013;61:1134–1145. DOI: 10.1002/glia.22502.
46. Bai JZ, Lipski J. Involvement of TRPV4 channels in Abeta(40)-induced hippocampal cell death and astrocytic Ca(2+) signalling. *Neurotoxicology*. 2014;41:64–72. DOI: 10.1016/j.neuro.2014.01.001.
47. Milosevic M, Stenovec M, Kreft M, Petrusic V, Stevic Z, Trkov S, Andjus PR, Zorec R. Immunoglobulins G from patients with sporadic amyotrophic lateral sclerosis affects cytosolic Ca2+ homeostasis in cultured rat astrocytes. *Cell Calcium*. 2013;54:17–25. DOI: 10.1016/j.ceca.2013.03.005.
48. Fernandes J, Lorenzo IM, Andrade YN, Garcia-Elias A, Serra SA, Fernandez-Fernandez JM, Valverde MA. IP3 sensitizes TRPV4 channel to the mechano- and osmotransducing messenger 5'-6'-epoxyeicosatrienoic acid. *J Cell Biol*. 2008;181:143–155. DOI: 10.1083/jcb.200712058.
49. Saxena A, Bachelor M, Park YH, Carreno FR, Nedungadi TP, Cunningham JT. Angiotensin II induces membrane trafficking of natively expressed transient receptor potential vanilloid type 4 channels in hypothalamic 4B cells. *Am J Physiol Regul Integr Comp Physiol*. 2014;307:R945–R955. DOI: 10.1152/ajpregu.00224.2014.
50. Mercado J, Baylie R, Navedo MF, Yuan C, Scott JD, Nelson MT, Brayden JE, Santana LF. Local control of TRPV4 channels by AKAP150-targeted PKC in arterial smooth muscle. *J Gen Physiol*. 2014;143:559–575. DOI: 10.1085/jgp.201311050.
51. Liu G, Hosomi N, Hitomi H, Pelisch N, Fu H, Masugata H, Murao K, Ueno M, Matsumoto M, Nishiyama A. Angiotensin II induces human astrocyte senescence through reactive oxygen species production. *Hypertens Res*. 2011;34:479–483. DOI: 10.1038/hr.2010.269.
52. Hong JH, Moon SJ, Byun HM, Kim MS, Jo H, Bae YS, Lee SI, Bootman MD, Roderick HL, Shin DM, et al. Critical role of phospholipase Cgamma1 in the generation of H_2O_2-evoked [Ca2+]i oscillations in cultured rat cortical astrocytes. *J Biol Chem*. 2006;281:13057–13067. DOI: 10.1074/jbc.M601726200.
53. Girouard H, Park L, Anrather J, Zhou P, Iadecola C. Angiotensin II attenuates endothelium-dependent responses in the cerebral microcirculation through nox-2-derived radicals. *Arterioscler Thromb Vasc Biol*. 2006;26:826–832. DOI: 10.1161/01.ATV.0000205849.22807.6e.
54. Crespo-Castrillo A, Arevalo MA. Microglial and astrocytic function in physiological and pathological conditions: estrogenic modulation. *Int J Mol Sci*. 2020;21:3219. DOI: 10.3390/ijms21093219.

SUPPLEMENTAL MATERIAL

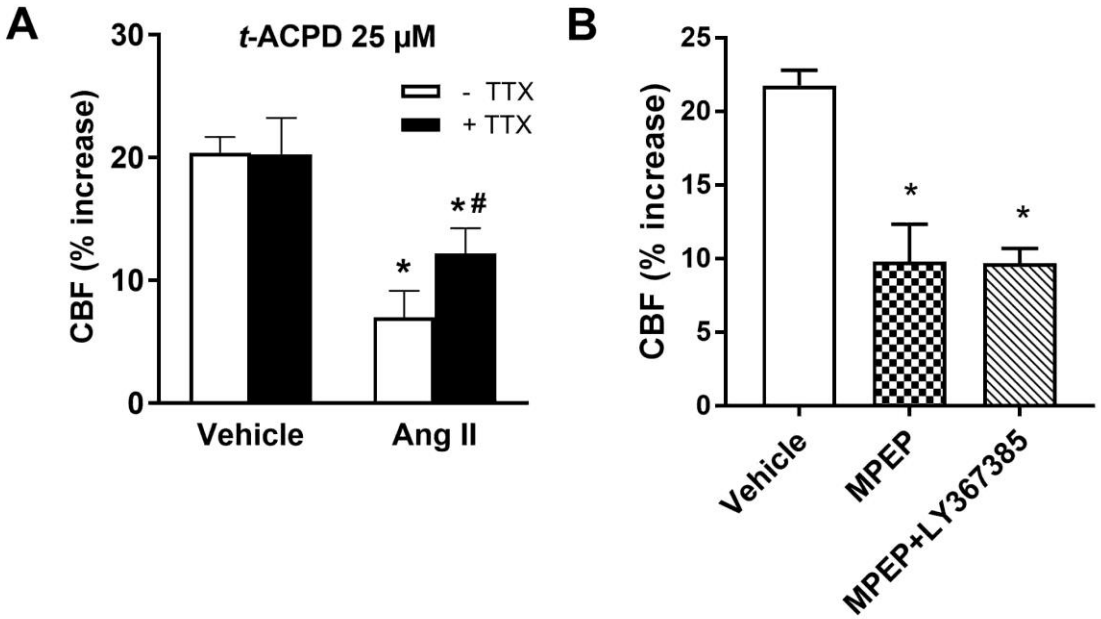

Supplemental Figure 1: Cerebral blood flow regulation by mGluRs in the somatosensory cortex. (A) Effects of 30 minutes superfusion with Angiotensin (Ang) II (50 nM) or its vehicle (aCSF) on the cerebral blood flow (CBF) increase in response to the mGluR agonist (1S,3R)-1-aminocyclopentane-1,3-dicarboxylic acid (t-ACPD, 5 minutes, 25 µM) superfused in the presence or absence of tetrodotoxin (TTX, 3 µM) (*$p<0.05$ compared to the respective vehicle, #$p<0.05$ compared to Ang II - TTX; two-way ANOVA followed by Tukey correction, n=4-6); (B) Effects of the specific metabotropic glutamate receptors 1 (mGluR1) and 5 (mGluR5) antagonists (2-methyl-6-(phenylethynyl)pyridine hydrochloride (MPEP; 30 µM) and (S)-(+)-alpha-amino-4-carboxy-2-methylbenzene-acetic acid (LY367385; 500 µM) on the CBF increase in response to whisker stimulation. MPEP and LY367385 were superfused during 20 minutes prior to the second series of whisker stimulations. Vehicle corresponds to the first series of whisker stimulations, (*$p<0.05$ compared to vehicle; one-way ANOVA followed by Tukey correction, n=2).

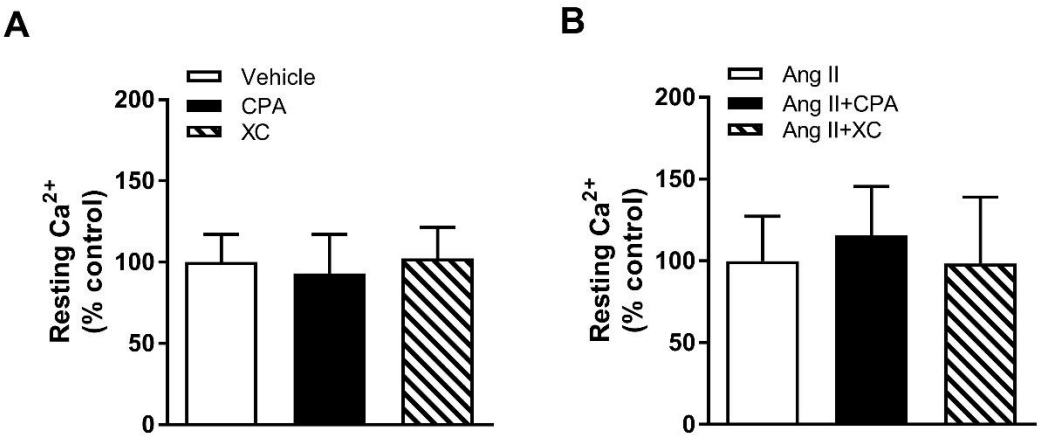

Supplemental Figure 2: IP3Rs and TRPV4 channels do not mediate Ang II action on resting astrocytic endfoot Ca2+ levels. Estimated [Ca2+]i at resting state presented in % of control in brain slices perfused with (A) the vehicle with or without the sarcoplasmic reticulum (SR)/ER Ca2+ ATPase (SERCA) inhibitor, cyclopiazonic acid (CPA; 30 μM) or the partial IP3Rs inhibitor, xestospongin C (XC, 10 μM); n=3-5; (B) Ang II (100 nM) alone with or without CPA (30 μM) or XC (10 μM), (one-way ANOVA followed by Tukey correction, n=5-6).